- 1 **Title:** A weather surveillance radar view of Alaskan avian migration
- 2 **Authors:** Ashwin Sivakumar<sup>1\*</sup>, Daniel Sheldon<sup>2</sup>, Kevin Winner<sup>2,3,4</sup>, Carolyn S. Burt<sup>5</sup>, Kyle G.
- 3 Horton<sup>5\*</sup>

4 5

#### **Affiliations:**

- 6 <sup>1</sup>Flintridge Preparatory School, La Cañada Flintridge, CA, USA
- <sup>7</sup> <sup>2</sup>College of Information and Computer Sciences, University of Massachusetts, Amherst, MA,
- 8 USA
- 9 <sup>3</sup>Ecology and Evolutionary Biology, Yale University, New Haven, CT, USA
- 10 <sup>4</sup>Center for Biodiversity and Global Change, Yale University, New Haven, CT, USA
- <sup>5</sup>Department of Fish, Wildlife, and Conservation Biology, Colorado State University, Fort
- 12 Collins, CO, USA
- \*Corresponding author, 22sivakumara@flintridgprep.org, kyle.horton@colostate.edu

14 15

33

34

35

36 37

38

39

40

41

42 43

44

- Keywords: aeroecology, Alaska, bird migration, macroecology, radar, remote sensing
- 16 **Abstract**: Monitoring avian migration within subarctic regions of the globe poses logistical challenges. Populations in these regions often encounter the most rapid effects of changing 17 18 climates, and these seasonally productive areas are especially important in supporting bird 19 populations — emphasizing the need for monitoring tools and strategies. To this end, we 20 leverage the untapped potential of weather surveillance radar data to quantify active 21 migration through the airspaces of Alaska. We use over 400,000 NEXRAD radar scans from seven stations across the state between 1995 and 2018 (86% of samples derived from 2013 22 23 to 2018) to measure spring and fall migration intensity, phenology, and directionality. A 24 large bow-shaped terrestrial migratory system spanning the southern two-thirds of the state 25 was identified, with birds generally moving along a northwest-southeast diagonal axis east 26 of the 150th meridian, and along a northeast-southwest axis west of this meridian. Spring 27 peak migration ranged from May 3<sup>rd</sup> to May 30<sup>th</sup> and between August 18<sup>th</sup> and September 28 12<sup>th</sup> during the fall, with timing across stations predicted by longitude, rather than latitude. 29 Across all stations, the intensity of migration was greatest during the fall as compared to spring, highlighting the opportunity to measure seasonal indices of net breeding 30 31 productivity for this important system as additional years of radar measurements are 32 amassed.

#### 1) Introduction

A detailed understanding of avian migratory behavior, especially regarding distribution and timing, is critical for the success of strategic conservation measures [1]. Historically, most research on avian migration has depended heavily on labor-intensive field techniques, including observational surveys as well as the capture of birds for banding, GPS tagging, or stable isotope analysis, focusing on studying migratory behavior of populations of individual species [2–5]. Indeed, many significant breakthroughs in migration ecology over the past decades have involved identifying migratory behavior of individual species or populations. This includes the discovery of the long-distance nonstop migration of Bar-tailed Godwits [6] using satellite telemetry and the discovery of "leap-frog migration" in Wilson's Warblers using stable isotope analysis [7]. While such techniques have substantially bolstered our understanding of migration dynamics, thus far, traditional species-by-species

tracking approaches have not lent themselves to holistic macro-level ecological insights [8]. Monitoring at this scale is challenged by magnitude, diversity, and scale, with avian migration patterns involving millions of individuals across flyways composed of hundreds of species and movements spanning thousands of kilometers [9,10]. This challenge is compounded especially in remote, inaccessible, or under-surveyed areas where field techniques have been insufficient in documenting macro-scale migratory trends and is thus especially pronounced in subarctic regions like Alaska.

Arctic and subarctic regions are seeing drastic ecological changes [11], including rapid shifts in flora, fauna, and climate [12–14], increasing the need for monitoring in these remote areas. Alaska and its surrounding waters are home to incredibly productive ecosystems, with the northern Bering and Chukchi seas being some of the most productive marine ecosystems on Earth [15]. Driven by long polar spring and summer days, terrestrial ecosystems in Alaska are similarly productive during the summer months, with remotely-sensed indices of greenness (e.g., normalized difference vegetation index) being higher in parts of Alaska during the summer than in most other regions of the planet [16]. This productivity, in combination with a relative low density of predators [17], makes Alaska a globally important destination for breeding birds [18]. However, the seasonal nature of Alaska's productivity means that the vast majority of breeding bird species in the state are migratory. This, combined with Alaska's unique geographic position as an ecological bridge between North America and Asia, with at least 1.5 million birds moving from Asia into Alaska every year [19], and as the northern border to the Pacific Ocean, makes Alaska a critical region to monitor avian migration.

In recent years, there has been a surge of interest in the use of radar remote-sensing to quantify region scale avian migration (e.g., Dokter et al., 2018; Horton et al., 2020; Horton, Van Doren, Stepanian, Farnsworth, & Kelly, 2016; Newcombe et al., 2019; Nilsson et al., 2019). In North America, however, these investigations have largely been confined to the contiguous United States (e.g., Van Doren & Horton, 2018). The reason for this constraint is largely due to infrastructure, with large-scale weather surveillance radars being more abundant in the contiguous U.S. and data spanning a longer period than anywhere else in North America or the world. In total, 143 radars reside in the contiguous U.S., with data spanning more than 25 years. Both Canada and Mexico operate similar radars, yet data access is more restricted and radar density is much lower. For example, Canada operates approximately 33 weather surveillance radars, with the majority of stations residing along the U.S.-Canada border — thus leaving most subarctic regions unmonitored by these tools. While small-scale radars have been deployed to analyze migratory movements in Alaska, efforts have been episodic [26], restricting their utility for long-term monitoring, and at times lending important but site-specific inferences (e.g., [27]).

To date, there have been no radar-based studies analyzing migration at a macro-scale in Alaska to determine how, when, and where birds move through the airspace. Yet while studies remain absent, weather surveillance radar data from seven NEXRAD weather surveillance stations distributed across Alaska have collected data for as many as 13 years. In this study, we resolve this gap by assembling all available NEXRAD data to quantify the intensity, timing, and directionality of avian migration across the region during spring and fall migratory seasons.

# 2) Methods

# (a) Weather surveillance radar

To quantify the timing, intensity, and directionality of migratory birds throughout portions of Alaska, we downloaded NEXRAD level-II data from seven radar stations (see Figure S1). We processed all nocturnal radar scans from April 1st to October 15th from 1995 to 2018. Data were downloaded from the Amazon Web Services repository (<a href="https://s3.amazonaws.com/noaa-nexrad-level2/index.html">https://s3.amazonaws.com/noaa-nexrad-level2/index.html</a>). While some samples were available in 1995 to 2003, 86% of our samples were derived from 2013 to 2018 — Alaskan radar data are not present in the NOAA archive from 2004 to 2012. See Figure S1 for individual radar data density metrics. For seasonal summaries, we defined spring from April 1st to July 1st and fall from July 15th to October 15th.

Radar scans are collected every 5 to 10 minutes depending on whether the radar is sampling precipitation (every 5 minutes) or sampling clear air (every 10 minutes). For each radar scan, we first identified and removed precipitation contamination across the five lowest radar tilt elevation scans ( $\sim$ 0.5°, 1.5, 2.5, 3.5, and 4.5°) using the MISTNET algorithm in the WSRLIB package of MATLAB [28,29]. Pixels characterized as containing precipitation contamination were set to zero. For each year, we applied a clutter mask to mitigate the impact of stationary contamination such as mountains, building, or persistent sea clutter. We built our annual clutter masks by summing a minimum of 100 low-elevation scans (0.5°), starting on 1 January (16:00 UTC to 18:00 UTC) and continuing to 15 January. We used these dates and times because they are not coincident with migration and would thus be free of biological signals. We classified any pixel above the 85th percentile of the summed reflectivity as clutter and masked these pixels from our analyses. For some early years, insufficient data were present to generate robust clutter masks, necessitating the use of more recent years of January data (e.g., PACG 1997 data used a mask from 2015). Otherwise, year specific clutter masks were used.

Next, from our precipitation free scans, we generated profiles of migratory activity, with migratory intensity quantified from reflectivity and migratory track and ground speed quantified from radial velocity. For these measures, data between 5 km and 100 km from the radar station were used, and profiles were output in 100 m intervals from 0-3km above ground level (generated from the five lowest radar tilt elevations, see previous paragraph). We used reflectivity (η) as a measure of migrant intensity, which was calculated by converting reflectivity factor (Z) as follows: dBη = dBZ +  $\beta$ , where  $\beta$  = 10log10(10³π⁵|Km|²/λ⁴) [30]. For our applications, we converted dBη to linear units following  $\eta$  = 10<sup>dBη</sup>/<sub>10</sub>. We used an average WSR-88D wavelength ( $\lambda$ ) of 10.7 cm and |Km|² for liquid water of 0.93, the dielectric constant. We de-aliased radial velocity data following Sheldon et al. (2013) and subsequently fit velocity azimuth displays (VAD) to quantify migrant track and groundspeed.

For summary statistics, we summed vertical profiles of reflectivity ( $\eta$ ) to generate single values of migration intensity per radar scan. We used the average of scans between sunset and sunrise to characterize nightly activity (see exception on timing below). We fit a generalized additive model with the quasi-Poisson family to reflectivity (response) and ordinal date (predictor). We used the R *mgcv* package to generate GAM models for phenology measures [32]. We used the model prediction of reflectivity to generate average phenology

curves for each radar station. We calculated the date of peak migration as the date of the highest predicted activity during the respective spring and fall periods. We also calculated the date at which 10% and 90% of migratory activity passed each NEXRAD station. To summarize profiles of track (migration flight direction), we weighted directions by reflectivity ( $\eta$ ). We then summarized these measures with rose diagrams, which display the distribution of measurements from individual scans, rather than nightly averages. Rather than simply plotting the distribution of track directions (i.e., equal weights for all directions of radar scans), we weighted track measures by the sum of profile reflectivity to prioritize scans with greater migratory activity. To summarize the concentration of track directions, we used the R *CircStats* package to calculate rho, or the mean resultant vector length, for each radar station. Plainly, rho measures the track concentration, with 0 reflecting no concentration (omni-directional movements) and 1 equating to complete concentration (completely directional movements).

One of the challenges with characterizing nocturnal migration at such high latitudes was that a true nocturnal period was exceedingly short or could not be identified during all periods from April 1st to October 15th, specifically during the periods when the sun does not set (late spring to early fall). For all sites, a minimum 8-hour sampling period starting at local sunset was used to characterize aerial movements. For areas and dates where the sun did not set, namely radar stations PAEC, PABC, PAHG, and PAPD, we characterized the "nocturnal period" as an 8-hour period starting at the last true sunset. For example, at PABC, civil twilight (sun 6° below horizon) could not be defined from June 13th to June 29th. For this period, we sampled 8 hours after the last true sunset (June 12th). If the true nocturnal period was shorter than 8-hours, we sampled a minimum of 8-hours after evening civil twilight (Figure S2).

For all samples, we removed vertical profile bins (100 m intervals) with RMSE from VADs > 10 m/s, and airspeeds < 5 m/s and > 35 m/s to mitigate insect contamination [33] and reduce the influence of measures with airspeeds outside the expectation for nocturnally migrating birds. The VAD model estimates a velocity vector for each height bin and assumes all scatterers within the bin move with the same velocity, which results in a predicted radial velocity at each azimuth. Here, RMSE at a height bin is the roost-mean squared error of the actual radial velocity values compared to the predicted ones. We calculated airspeed using vector subtraction and derived wind speeds from the North American Regional Reanalysis [34]. NARR data are assembled at 3-hour temporal intervals, 32 km spatial resolution, and are modeled at 25 hPa vertical intervals. We calculated airspeed using vector subtraction from ground speed and track direction (derived from velocity azimuth displays). Following these filtering protocols, we only used profiles of activity if five of more height bins remained. These protocols are geared towards the capture of passage migrations, likely to be composed of small-bodied passerines, although waterfowl, shorebirds, and a small percentage of bats are expected to also reside within the signals. Low flying activities (below 100 m), whether of migratory birds or birds making foraging bouts, are not likely to be captured by these radar sensors.

All analyses and figures were generated using R version 4.0.2 [35].

#### 3) Results

(a) Intensity

In total, we utilized 401,272 radar scans across 1,840 sampling dates for our quantification of migration through Alaska. The highest migratory intensity in spring occurred at PACG (Sitka; Figure 2) and PAPD (Fairbanks), while the highest migratory intensity during fall was recorded at PAPD (Fairbanks) and PAHG (Anchorage). Compared to every other station, migratory intensity at PAEC (Nome) remained very low throughout the year (94.6% of observations < 50  $\eta$ , as compared to 45.9% < 50  $\eta$  for all other stations; Figure 2). All stations recorded higher peak migratory intensity in fall than in spring, and statewide, a significant difference in intensity between spring and fall was found (paired t-test, t<sub>6</sub> = 2.959, p = 0.025).

#### (b) Phenology

During spring, dates of peak migration ranged between May  $2^{nd}$  and May  $29^{th}$  and during fall, between August  $17^{th}$  and September  $11^{th}$  (Figure 2, Table 1). There was a negative relationship between longitude and date of peak migration in spring (slope=-0.861,  $R^2$ =0.785, p=0.008; Figure 3A) and a positive relationship in fall (slope=0.862,  $R^2$ =0.84, p=0.004; Figure 3B), indicating very strong westward migration in spring and very strong eastward migration in fall. We did not find a significant association between latitude and date of peak migration in spring ( $R^2$ =0.35, p=0.163; Figure S3A) or in fall ( $R^2$ =0.24, p=0.267, Figure S3B).

The time between spring and fall date of peak migration was greatest at PACG (Sitka, 131 days, Table 1), which was the southernmost and easternmost station; while the time between peaks was shortest at PAEC (Nome, 81 days, Table 1), which was the westernmost station. The average across the state was  $100.6\pm19.1(\pm SD)$  days. PAPD (Fairbanks), the northernmost station, experienced 100 days between spring and fall date of peak migration, essentially equal to the statewide average. Interval length was predicted by longitude (slope=1.725,  $R^2$ =0.84, p=0.004), but not latitude ( $R^2$ =0.31, p=0.201).

In addition to examining the seasonal date at which migration intensity peaked, we also defined the start (date at which the  $10^{th}$  quantile of summed activity occurred) and end (date at which the  $90^{th}$  quantile of summed activity occurred) of each migratory season. During spring, the start was earliest at PAIH (Middleton Island, April  $10^{th}$ ) and PACG (Sitka, April  $12^{th}$ ) and latest at PAKC (King Salmon, May  $1^{st}$ ) and PAPD (Fairbanks, May  $2^{nd}$ ). Conversely, spring end dates were earliest at PACG (Sitka, May  $27^{th}$ ) and PAPD (Fairbanks, May  $30^{th}$ ), and latest at PAEC (Nome, June  $17^{th}$ ). Interestingly, while the start dates during spring tended toward earlier dates at the easternmost locations, no statistically significant relationship between spring start dates and either longitude or latitude was detected (longitude,  $R^2$ =0.30, p=0.205; latitude  $R^2$ =0.24, p=0.266). However, the end of spring migration did show a strong relationship with longitude (slope=-0.611,  $R^2$ =0.81, p=0.006), but not latitude ( $R^2$ =0.19, p=0.327).

Analysis of fall start and end dates largely followed the opposite trends. Fall migration started earliest at PAEC (Nome, July 31<sup>st</sup>) and PABC (Bethel, August 2<sup>nd</sup>), and started latest at PAPD (Fairbanks, August 13<sup>th</sup>) and PACG (Sitka, August 14<sup>th</sup>). Conversely, fall migration ended earliest at PAKC (King Salmon, September 4<sup>th</sup>) and PAPD (Fairbanks, September 11<sup>th</sup>), and ended latest at PACG (Sitka, October 2<sup>nd</sup>) and PAIH (Middleton Island, October 2<sup>nd</sup>). Unlike in the spring, the beginning of fall migration had a strong relationship with longitude (slope=0.531, R²=0.89, p=0.001), but not latitude (R²=0.08, p=0.538). The end of fall

migration did not show a spatial relationship with longitude ( $R^2$ =0.17, p=0.347) or latitude ( $R^2$ =0.06, p=0.592).

Overall, migration in Alaska was characterized as possessing substantial and significant east-west directionality, but no significant north-south directionality.

#### (c) Directionality

For each station, we summarized the seasonal distribution of migrant track directions (Figure 3), mean migration track, and rho, a measure of the track concentration (0 = no concentration, 1 = complete concentration; Table 1). Of the stations, PACG, near Sitka, was the only one that exhibited typical north-south migratory directionality — namely, predominantly northwesterly migration during the spring (316.57 degrees, rho = 0.89) and predominantly southeasterly migration during the fall ( $152.16^\circ$ , rho = 0.66).

The remainder of stations showed patterns that were largely unique to Alaska's geography. For example, PABC, PAKC, PAHG, three southwestern Alaskan stations, showed northeasterly migration in the spring and southwesterly migration in the fall. PAPD, near Fairbanks, exhibited west-northwesterly migration in spring (mean  $290.48^{\circ}$ , rho = 0.92) and easterly migration in fall ( $92.49^{\circ}$ , rho = 0.95). PAIH, on Middleton Island (Figure 1), exhibited both west-northwesterly and east-northeasterly migration in spring ( $20.82^{\circ}$ , rho = 0.21; Figure 3A), with this bimodal distribution of migratory directionality making the track direction misleading; but primarily northeasterly migration in the fall ( $80.02^{\circ}$ , rho = 0.74; Figure 3B). PAEC, near Nome, appeared to exhibit westerly migratory directionality in spring ( $265.27^{\circ}$ ) and northwesterly directionality in fall ( $317.36^{\circ}$ ). However, the low rho values of 0.27 and 0.13 in spring and fall, respectively, as well as the extremely low migratory volume detected by PAEC annually, mean that these observed trends should not be taken as a meaningful representation of migratory directionality.

# 4) Discussion

Alaska is home to hundreds of avian species, with the majority of those species being migratory [26,36,37]. As a breeding destination for many species, species departing Alaska travel to as many as six different continents to reach their wintering destinations [6,38,39] — a phenomenon that connects distant parts of our global ecosystem. Using NEXRAD weather surveillance data, we quantified spring and fall avian migration throughout Alaska, documenting patterns of phenology, abundance, and behavior. With increased pressure due to anthropogenic development and climate change, it is important that we have tools ready for understanding how migration systems adapt to local or distant environmental changes.

In both spring and fall, average migratory intensity was highest at the easternmost stations (near Sitka and Fairbanks), with average intensity progressively decreasing for stations further to the west. This trend can be explained by the majority of terrestrial migrants in Alaska entering the region in spring and leaving the region in fall from the east. Importantly, as predicted, migratory intensity at every station was higher in fall than in spring (mean of 144% increase), a difference which can be largely attributed to breeding activity, as fall migration includes not only the after-hatch-year birds which arrived in spring, but also hatch-year juveniles. Previous research from the contiguous United States [20] has shown the value of using seasonal differences in migratory biomass to evaluate rates of survival. In the same vein, the size of the difference in intensity between spring and fall migration within the Alaskan system may be used as a relative indicator of breeding

productivity in the region — the greater the number of juvenile birds produced, the greater the intensity of fall migration will be compared to spring migration. Moving forward, variation in these metrics will be important in understanding the impacts of natural and anthropogenic change of bird populations, including drought, forest fires, severe weather, or changes in phenology [40].

While many aerial migratory systems are often contextualized as north-south progressing movements (e.g., [21,24,41]), we found that date of peak migratory intensity was strongly and significantly associated with longitude, with the association being negative in spring and positive in fall. We did not find a significant relationship of date of peak migratory intensity with latitude during the spring or fall. These findings point to an overall westward migration in spring and eastward migration in fall, which dominates any smaller-scale signal of north-south phenology — an expected result given the region's east-west peninsular geography. Predictably, the time between spring and fall date of peak migration was greater at stations further east and predicted by longitude, rather than latitude. However, PAPD (Fairbanks), one of the easternmost stations, had a much shorter interval between spring and fall date of peak migration than other stations in eastern Alaska. This deviation is likely explained by a northwest-southeast axis of migration within the eastern portion of the state, which means that more northern, inland locations receive migrants later in spring and earlier in fall than other sites at their same longitude despite the absence of an overall regional relationship between dates of peak migration and latitude.

Analysis of migratory tracks revealed a "bow-shaped" pattern of migratory directionality (Figure 4). In spring, migration east of the 150th meridian was primarily northwesterly, while west of the meridian, it was primarily southwesterly. The exception to this trend was Middleton Island, which recorded two primary directions of migration in spring — northwest and northeast. The northeastern movement, which differs from the trend in the rest of eastern Alaska, may be attributed to seabirds moving from the open ocean into the Gulf of Alaska. In fall, only the easternmost station (PACG, Sitka), recorded primarily southeastern migratory directionality. Fairbanks, on the other hand, recorded primarily easterly migration, and every other station recorded northeasterly migration. Thus, the point at which the overall mass of migrating birds switches from migrating along one diagonal axis to migrating along the other is located further east during the fall than during the spring. This finding suggests that fall migration in Alaska is geographically distinct, rather than simply being a reversal of spring migration. More specifically, fall migration appears to occur, on aggregate, further inland than spring migration. In the western contiguous USA, migrants maximize survival and breeding success by using lower elevation, more ecologically productive coastal areas during the spring, while minimizing distance traveled during the fall by using higher elevation inland areas [44]. Our results suggest that migrants generally use this strategy in Alaska as well.

Curiously, while our results showed a strong relationship between longitude and both the end of spring migration and the beginning of fall migration, we did not find a significant relationship between either latitude or longitude with the beginning of spring migration and the end of fall migration. One hypothesis may be that the dates of spring thaw and first frost in autumn are determined as much by topography as by latitude or longitude. Thus, as a consequence of Alaska's complex montane geography, areas likely transition in and out of suitability for breeding birds in an order that is not closely related to either latitude or longitude. Further site-specific investigation will be necessary in order

to evaluate the relative contributions of latitude, longitude, and topography on the beginning of spring migration and the end of fall migration.

318

319

320

321

322

323

324

325

326

327

328

329

330

331

332

333

334

335

336337

338

339

340

341

342

343

344

345

346

347

348

349

350

351

352

353

354

355

356357

358

359

360

361

362

Our overall finding of a bow-shaped migration in both spring and fall, with the vertex of the bow located further to the east in fall than in spring, complements the findings of previous studies of migration in Alaska, both radar-based and focused on individual species. One radar study [26] characterized a polar migration system involving more than 2 million seabirds and shorebirds moving along and near the Arctic coastline, frequently between North America and Asia, from July to August. The most salient feature of the Alaskan section of this system was heavy southeasterly movement into the northwest coast of Alaska (between the Seward Peninsula and Utqiagvik). Our analysis found that southwestern Alaska experiences primarily northeasterly migration in the fall; the contrast between migratory directionality in northwestern and southwestern Alaska suggests that the polar coastal system of migration in the northern third of the state is largely distinct from the bow-shaped migratory system that dominates the state south of the Arctic Circle. Another radar analysis [27], while focusing on the altitude of migrating birds in the upper Tanana valley in east-Central Alaska, also reported that the vast majority of observed bird movement was westerly and northwesterly in spring and easterly or northeasterly in fall. Our results for the PAPD station near Fairbanks (which lies within the Tanana valley) corroborate these findings. A recent large-scale analysis of American Robin (Turdus migratorius) spring migration in northwestern North America using GPS tagging [45] found that American Robins enter Alaska from the east in a northwesterly fashion, but the majority of tagged birds that continued migrating beyond the state's eastern borderlands quickly switched to westerly or southwesterly migration in order to reach breeding habitat in southern and south-central Alaska. These findings support that individual passerine species exhibit the same bowshaped migration that characterizes the aggregate terrestrial migratory activity in the state.

In addition to quantifying broadscale migration patterns, our approach also reveals site-specific migration dynamics, complementing prior localized studies of migration in Alaska. Middleton Island in the Gulf of Alaska recorded substantial migration in both spring and fall (Figure 1), consistent with trends on the mainland. The island's long record as a migratory stopover site [37] points to a large-scale landbird migration system over the Gulf of Alaska and the North Pacific in both spring and fall. Massive landbird migration systems over the Gulf of Mexico and Mediterranean Sea have been extensively documented [46,47], but a potentially analogous system in the North Pacific has yet to be fully characterized. A field-based analysis of forest passerine migration in the Fairbanks area recorded a period of 105 days between spring and fall peak migration [48]. This finding is closely matched by our results, which indicate a period of 100 days between spring and fall peak migration for Fairbanks. The similarity of these two values, despite the fact that the earlier study solely recorded data for 18 passerine species, suggests either that non-passerines in the region migrate in rough temporal synchrony with passerines, possibly due to a narrow window of food availability, or that they account for a relatively small proportion of the local migratory biomass. Additionally, our intervals between spring and fall, while predictably shorter than those of the contiguous US (mean 146.8±12.6, days±SD [21]), follow a macroscale pattern of decreasing intervals with increasing latitude. Examining the contiguous US, we see that the interval between spring and fall decreases 1.5 days/°latitude. By way of extrapolation, we predicted intervals between spring and fall in Alaska would range between 118.5 days (site

PACG, 56.5°N, true interval measured at 131 days) and 106.5 days (site PAPD, 65.0°N, true interval measured at 100 days) — patterns that are broadly reflected in our data.

Lastly, our analysis highlights a wealth of opportunities for future research concerning macro-scale migration in Alaska. One key priority for migration research, especially in subarctic regions such as Alaska, is understanding the impact of climate change on migratory behavior, particularly with regard to migration phenology [21,45,49]. For example, previous theoretical work [42] explains that the east-west migratory axis of Asian species breeding in Alaska means that even slight increases in the duration of summer productivity due to climate change would allow those species to penetrate further into Alaska's interior by giving them slightly more temporal leeway to migrate further along the axis. While Asian "crossover" species probably only account for a very small proportion of migratory birds in Alaska today [43], our finding of overwhelming east-west directionality in the Alaskan migratory system confirms that Beringia may become the stage for rapid intercontinental range expansion of both Asian and North American species. Moreover, as more years of data accrue within the NEXRAD archive, beyond the recent 5-7 years of data that represent the core of our findings, statistical inferences will be able to be drawn from these time series. Station PAPD will serve as an important benchmark for these future studies, currently with 13 years of data spanning 24 years; each passing season will contribute an annual replicate of freely accessible radar data. These next steps will be enhanced by the integration of community science observations, such as eBird [50], to refine estimates of phenology, intensity, and directionality [10,51]. Our current analysis does not incorporate species composition, which varies substantially across the region. For example, the proportion of shorebirds and waterfowl within the system is likely far higher at coastal stations than at inland ones. Understanding the different composition of migrating birds in different parts of the state is important for prioritizing habitat conservation projects and understanding critical indices of change.

388 389

390

363

364

365

366367

368

369

370

371

372

373

374

375

376

377

378

379

380

381

382

383

384

385

386

387

- **Ethics:** Approval was not required for this study.
- **Data accessibility:** The dataset is provided as electronic supplementary material.
- 392 **Authors' contributions:** AS and KGH conceived the study design and analyses. DS and KW
- 393 processed NEXRAD radar data. KGH and CSB designed figures. All authors provided edits and
- 394 comments.
- 395 **Competing interests:** We declare we have no competing interests.
- 396 **Acknowledgements:** Funding for this project was provided by NSF DBI-1661259 and NSF
- 397 MSB-NES-2017554. We thank Kevin Winker and Greg Mitchell for constructive and
- thoughtful commentary on an earlier version of this manuscript.

#### References:

- 1. Faaborg J *et al.* 2010 Conserving migratory land birds in the New World: Do we know enough? *Ecol. Appl.* **20**, 398–418. (doi:10.1890/09-0397.1)
- 404 2. Kelly JF, Finch DM. 1998 Tracking migrant songbirds with stable isotopes. *Trends in Ecology and Evolution* **13**, 48–49.
- 3. Bridge ES, Kelly JF, Contina A, Gabrielson RM, MacCurdy RB, Winkler DW. 2013
   Advances in tracking small migratory birds: a technical review of light-level
   geolocation. *Journal of Field Ornithology* 84, 121–137. (doi:10.1111/jofo.12011)
- 409 4. Bouten W, Baaij EW, Shamoun-Baranes J, Camphuysen KCJ. 2013 A flexible GPS tracking system for studying bird behaviour at multiple scales. *J Ornithol* **154**, 571–580. (doi:10.1007/s10336-012-0908-1)
- Handel CM, Sauer JR. 2017 Combined analysis of roadside and off-road breeding bird
   survey data to assess population change in Alaska. *cond* 119, 557–575.
   (doi:10.1650/CONDOR-17-67.1)
- Gill RE *et al.* 2009 Extreme endurance flights by landbirds crossing the Pacific Ocean:
   ecological corridor rather than barrier? *Proceedings of the Royal Society of London B: Biological Sciences* 276, 447–457. (doi:10.1098/rspb.2008.1142)
- 7. Paxton KL, Van Riper C, Theimer TC, Paxton EH. 2007 Spatial and Temporal Migration Patterns of Wilson's Warbler (Wilsonia Pusilla) in the Southwest as Revealed by Stable Isotopes. *Auk* **124**, 162–175. (doi:10.1093/auk/124.1.162)
- 8. Kelly JF, Horton KG. 2016 Toward a predictive macrosystems framework for migration ecology. *Global Ecol. Biogeogr.* **25**, 1159–1165. (doi:10.1111/geb.12473)
- 423 9. La Sorte FA, Fink D, Hochachka WM, DeLong JP, Kelling S. 2013 Population-level scaling
   424 of avian migration speed with body size and migration distance for powered fliers.
   425 *Ecology* 94, 1839–1847. (doi:10.1890/12-1768.1)
- 426 10. Horton KG, Van Doren BM, La Sorte FA, Cohen EB, Clipp HL, Buler JJ, Fink D, Kelly JF,
   427 Farnsworth A. 2019 Holding steady: Little change in intensity or timing of bird
   428 migration over the Gulf of Mexico. *Global Change Biology* 25, 1106–1118.
   429 (doi:10.1111/gcb.14540)
- 430 11. Høye TT, Post E, Meltofte H, Schmidt NM, Forchhammer MC. 2007 Rapid advancement
  431 of spring in the High Arctic. *Current Biology* 17, R449–R451.
  432 (doi:10.1016/j.cub.2007.04.047)
- 433 12. Zhang X, Sorteberg A, Zhang J, Gerdes R, Comiso JC. 2008 Recent radical shifts of atmospheric circulations and rapid changes in Arctic climate system. *Geophysical Research Letters* **35**. (doi:https://doi.org/10.1029/2008GL035607)

- 436 13. Tape KD, Hallinger M, Welker JM, Ruess RW. 2012 Landscape Heterogeneity of Shrub
- 437 Expansion in Arctic Alaska. *Ecosystems* **15**, 711–724. (doi:10.1007/s10021-012-9540-
- 438 4)
- 439 14. Pearson RG, Phillips SJ, Loranty MM, Beck PSA, Damoulas T, Knight SJ, Goetz SJ. 2013
- Shifts in Arctic vegetation and associated feedbacks under climate change. *Nature*
- 441 *Climate Change* **3**, 673–677. (doi:10.1038/nclimate1858)
- 442 15. Grebmeier JM *et al.* 2006 A Major Ecosystem Shift in the Northern Bering Sea. *Science*
- 443 **311**, 1461–1464. (doi:10.1126/science.1121365)
- 16. Ji D-B, Shi J-C, Letu H, Wang T-X, Zhao T-J. 2017 Atmospheric Effect Analysis and
- 445 Correction of the Microwave Vegetation Index. *Remote Sensing* **9**, 606.
- 446 (doi:10.3390/rs9060606)
- 17. DeGregorio BA, Chiavacci SJ, Benson TJ, Sperry JH, Weatherhead PJ. 2016 Nest
- 448 Predators of North American Birds: Continental Patterns and Implications. *BioScience*
- **66**, 655–665. (doi:10.1093/biosci/biw071)
- 450 18. Gill RE Jr, Handel CM. 1990 The Importance of Subarctic Intertidal Habitats to
- 451 Shorebirds: A Study of the Central Yukon-Kuskokwim Delta, Alaska. *The Condor* **92**,
- 452 709–725. (doi:10.2307/1368690)
- 453 19. Winker K, Gibson DD. 2010 The Asia-to-America influx of avian influenza wild bird
- 454 hosts is large. *Avian Dis* **54**, 477–482. (doi:10.1637/8741-032509-Reg.1)
- 20. Dokter AM, Farnsworth A, Fink D, Ruiz-Gutierrez V, Hochachka WM, Sorte FAL,
- Robinson OJ, Rosenberg KV, Kelling S. 2018 Seasonal abundance and survival of North
- 457 America's migratory avifauna determined by weather radar. *Nature Ecology & Evolution*
- 458 **2**, 1603–1609. (doi:10.1038/s41559-018-0666-4)
- 459 21. Horton KG, La Sorte FA, Sheldon D, Lin T-Y, Winner K, Bernstein G, Maji S, Hochachka
- 460 WM, Farnsworth A. 2020 Phenology of nocturnal avian migration has shifted at the
- 461 continental scale. *Nature Climate Change* **10**, 63–68. (doi:10.1038/s41558-019-0648-9)
- 462 22. Horton KG, Van Doren BM, Stepanian PM, Farnsworth A, Kelly JF. 2016 Seasonal
- differences in landbird migration strategies. *Auk* **133**, 761–769.
- 23. Newcombe PB, Nilsson C, Lin T-Y, Winner K, Bernstein G, Maji S, Sheldon D, Farnsworth
- A, Horton KG. 2019 Migratory flight on the Pacific Flyway: strategies and tendencies of
- wind drift compensation. *Biology Letters* **15**, 20190383. (doi:10.1098/rsbl.2019.0383)
- 467 24. Nilsson C *et al.* 2019 Revealing patterns of nocturnal migration using the European
- weather radar network. *Ecography* **42**, 876–886. (doi:10.1111/ecog.04003)
- 469 25. Van Doren BM, Horton KG. 2018 A continental system for forecasting bird migration.
- 470 *Science* **361**, 1115–1118. (doi:10.1126/science.aat7526)

- 471 26. Alerstam T, Bäckman J, Gudmundsson GA, Hedenström A, Henningsson SS, Karlsson H,
- Rosén M, Strandberg R. 2007 A polar system of intercontinental bird migration.
- 473 *Proceedings of the Royal Society B: Biological Sciences* **274**, 2523–2530.
- 474 (doi:10.1098/rspb.2007.0633)
- 475 27. Cooper BA, Ritchie RJ. 1995 The Altitude of Bird Migration in East-Central Alaska: A
- 476 Radar and Visual Study. *Journal of Field Ornithology* **66**, 590–608.
- 477 28. Lin T *et al.* 2019 MISTNET: Measuring historical bird migration in the US using archived
- weather radar data and convolutional neural networks. *Methods Ecol Evol* **10**, 1908–
- 479 1922. (doi:10.1111/2041-210X.13280)
- 480 29. Sheldon D. 2015 WSRLIB: MATLAB toolbox for weather surveillance radar. See
- 481 http://bitbucket.org/dsheldon/wsrlib.
- 482 30. Chilson PB, Frick WF, Stepanian PM, Shipley JR, Kunz TH, Kelly JF. 2012 Estimating
- animal densities in the aerosphere using weather radar: To Z or not to Z? *Ecosphere 3*,
- 484 art72. (doi:10.1890/ES12-00027.1)
- 485 31. Sheldon D, Farnsworth A, Irvine J, Van Doren B, Webb K, Dietterich TG, Kelling S. 2013
- 486 Approximate Bayesian inference for reconstructing velocities of migrating birds from
- 487 weather radar. *AAAI*, 1334–1340.
- 488 32. Wood SN. 2011 Fast stable restricted maximum likelihood and marginal likelihood
- 489 estimation of semiparametric generalized linear models. *Journal of the Royal Statistical*
- 490 Society: Series B (Statistical Methodology) **73**, 3–36. (doi:10.1111/j.1467-
- 491 9868.2010.00749.x)
- 492 33. Larkin RP. 1991 Flight speeds observed with radar, a correction: slow 'birds' are
- 493 insects. *Behav. Ecol. Sociobiol.* **29**, 221–224.
- 494 34. Mesinger F et al. 2006 North American Regional Reanalysis. Bull. Amer. Meteor. Soc. 87,
- 495 343–360. (doi:10.1175/BAMS-87-3-343)
- 496 35. R Core Team. 2020 R: A Language and Environment for Statistical Computing. Vienna,
- 497 Austria: R Foundation for Statistical Computing. See https://www.R-project.org/.
- 498 36. Johnson SR, Herter DR. 1990 Bird Migration in the Arctic: A Review. In *Bird Migration*
- 499 (ed PDE Gwinner), pp. 22–43. Springer Berlin Heidelberg.
- 37. DeCicco LH, Gibson DD, Tobish TG, Heinl SC, Hajdukovich NR, Johnson JA, Wright CW.
- 501 2017 Birds of Middleton Island, a unique landfall for migrants in the Gulf of Alaska.
- 502 *Western Birds* **48**, 214–293. (doi:doi 10.21199/WB48.4.1)
- 38. Bairlein F, Norris DR, Nagel R, Bulte M, Voigt CC, Fox JW, Hussell DJT, Schmaljohann H.
- 2012 Cross-hemisphere migration of a 25 g songbird. *Biology Letters* **8**, 505–507.
- 505 (doi:10.1098/rsbl.2011.1223)

- 39. Morris SR, Covino KM, Jacobs JD, Taylor PD. 2016 Fall migratory patterns of the Blackpoll Warbler at a continental scale. *The Auk* **133**, 41–51. (doi:10.1642/AUK-15-133.1)
- 40. Bauer S *et al.* 2019 The grand challenges of migration ecology that radar aeroecology can help answer. *Ecography* **42**, 861–875. (doi:10.1111/ecog.04083)
- 41. La Sorte FA *et al.* 2014 The role of atmospheric conditions in the seasonal dynamics of North American migration flyways. *J. Biogeogr.* **41**, 1685–1696.
- 513 (doi:10.1111/jbi.12328)
- 42. Winker K, Gibson DD. 2018 Some broad-scale effects of recent and future climate
- 515 change among migratory birds in Beringia. In *Trends and Traditions: Avifaunal Change*
- *in Western North America* (eds S W. David, Jr Robert E. Gill, H Collen M.), pp. 432–440.
- 517 Western Field Ornithologists.
- 43. Winker K *et al.* 2007 Movements of birds and avian influenza from Asia into Alaska. *Emerg Infect Dis* **13**, 547–552. (doi:10.3201/eid1304.061072)
- 519 Emery Inject Dis **13**, 547–552. (doi:10.5201/eid1504.061072)
- 520 44. La Sorte FA, Fink D, Hochachka WM, DeLong JP, Kelling S. 2014 Spring phenology of ecological productivity contributes to the use of looped migration strategies by birds.
- 522 *Proc. R. Soc. B* **281**, 20140984. (doi:10.1098/rspb.2014.0984)
- 45. Oliver RY, Mahoney PJ, Gurarie E, Krikun N, Weeks BC, Hebblewhite M, Liston G,
- Boelman N. 2020 Behavioral responses to spring snow conditions contribute to long-
- term shift in migration phenology in American robins. *Environ. Res. Lett.* **15**, 045003.
- 526 (doi:10.1088/1748-9326/ab71a0)
- 46. Biebach H, Biebach I, Friedrich W, Heine G, Partecke J, Schmidl D. 2000 Strategies of
- 528 passerine migration across the Mediterranean Sea and the Sahara Desert: a radar study.
- *Ibis* **142**, 623–634. (doi:https://doi.org/10.1111/j.1474-919X.2000.tb04462.x)
- 47. Cohen EB, Horton KG, Marra PP, Clipp HL, Farnsworth A, Smolinsky JA, Sheldon D, Buler
- JJ. 2021 A place to land: spatiotemporal drivers of stopover habitat use by migrating
- birds. *Ecology Letters* **24**, 38–49. (doi:https://doi.org/10.1111/ele.13618)
- 48. Benson A-M, Winker K. 2001 Timing of Breeding Range Occupancy Among High-
- latitude Passerine Migrants. *tauk* **118**, 513–519. (doi:10.1642/0004-
- 535 8038(2001)118[0513:T0BR0A]2.0.C0;2)
- 49. Buskirk JV, Mulvihill RS, Leberman RC. 2009 Variable shifts in spring and autumn
- 537 migration phenology in North American songbirds associated with climate change.
- 538 *Global Change Biology* **15**, 760–771. (doi:10.1111/j.1365-2486.2008.01751.x)
- 539 50. Sullivan BL *et al.* 2014 The eBird enterprise: an integrated approach to development
- and application of citizen science. *Biological Conservation* **169**, 31–40.
- 541 (doi:10.1016/j.biocon.2013.11.003)

51. Horton KG, Van Doren BM, La Sorte FA, Fink D, Sheldon D, Farnsworth A, Kelly JF. 2018 Navigating north: how body mass and winds shape avian flight behaviours across a North American migratory flyway. *Ecology Letters* **21**, 1055–1064. (doi:10.1111/ele.12971)

# **Figures and Tables:**

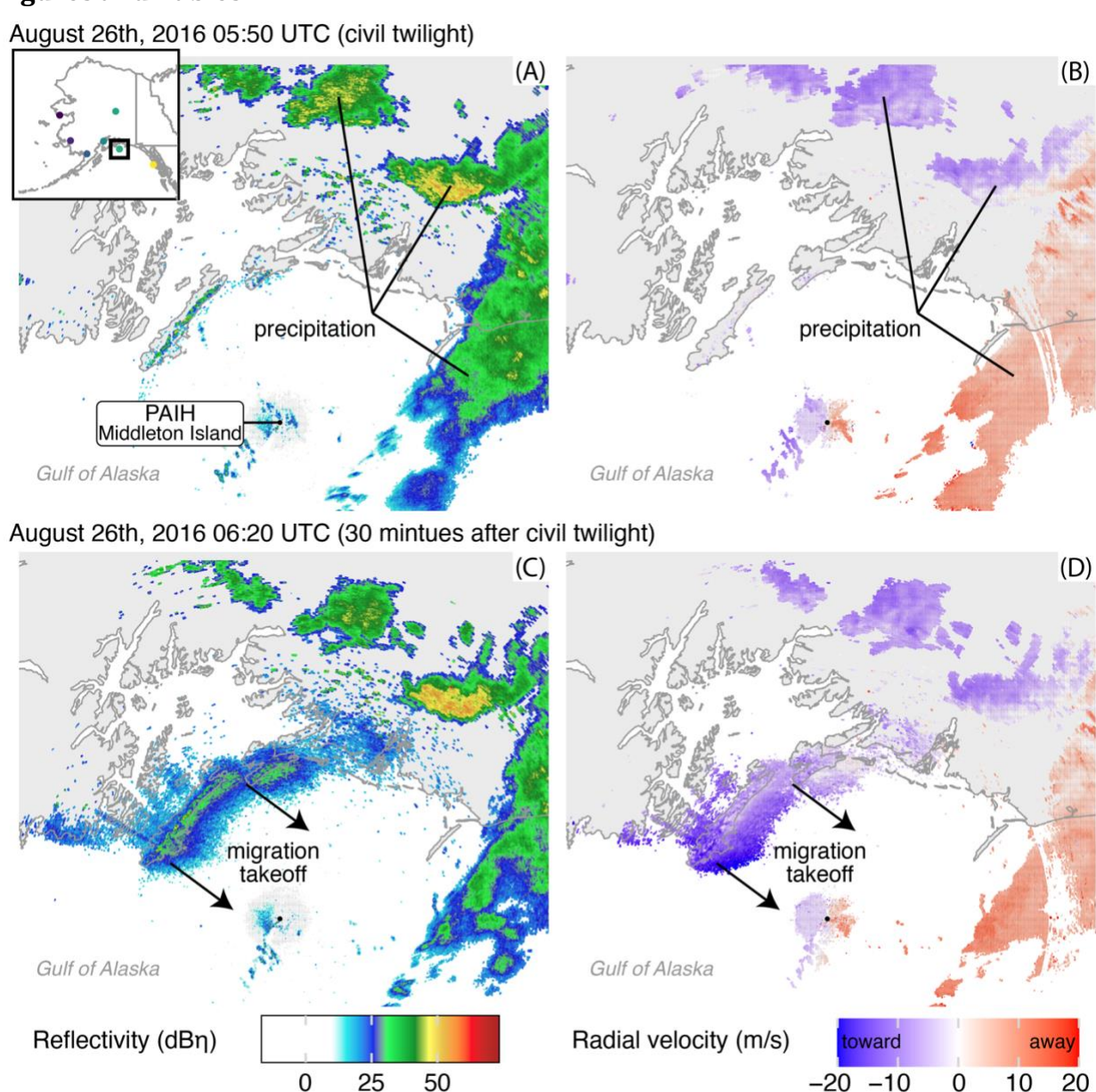


**Figure 1:** Radar measures of reflectivity (used to measure migration intensity) and radial velocity (used to measure migrant track) from NEXRAD station PAIH (Middleton Island, Alaska USA) from August 26<sup>th</sup>, 2016. **A** and **B** show measures taken at civil twilight (05:50 UTC) and **C** and **D** show measures taken 30 minutes after civil twilight, during which migration takeoff can be seen along coastal islands. In each of the images, precipitation contamination can be seen in the north and east. In our analysis, precipitation was removed using the MISTNET algorithm. Leftmost inset shows the locations of all seven NEXRAD stations, with the location of PAIH highlighted.

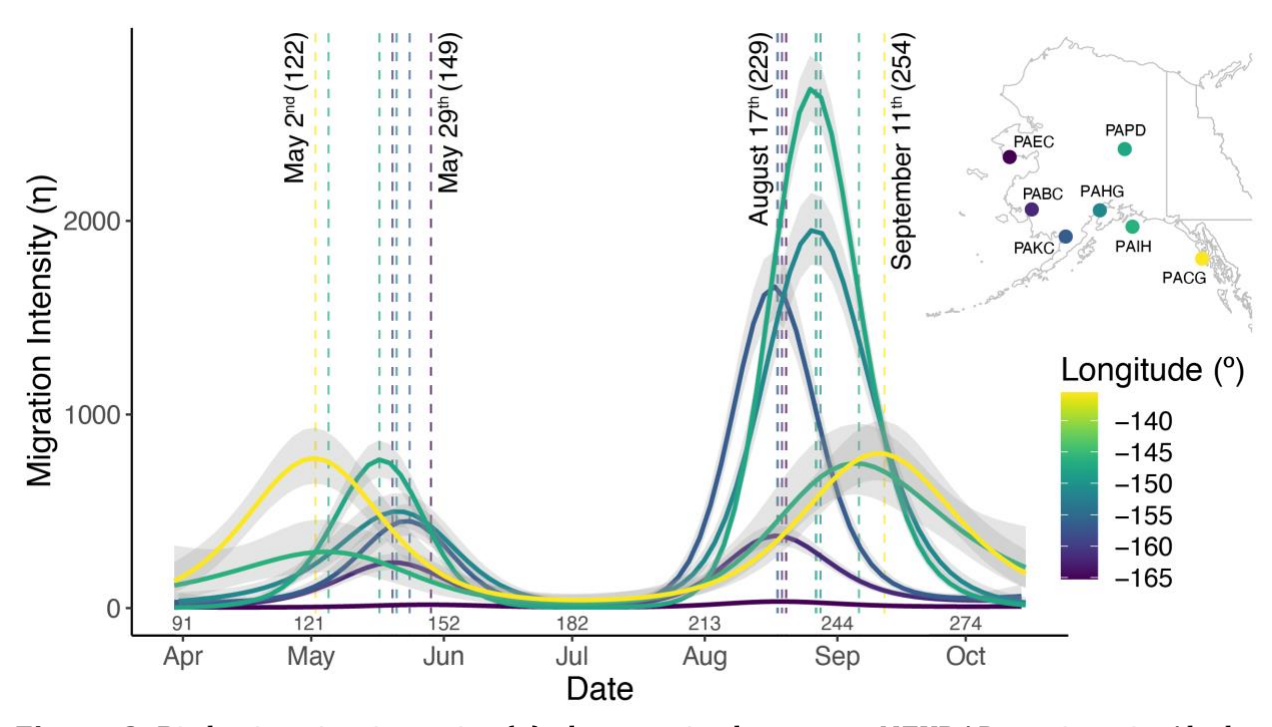


**Figure 2:** Bird migration intensity ( $\eta$ ) characterized at seven NEXRAD stations in Alaska, USA from 1995 to 2018. The fitted lines and 95% confidence bands are from generalized additive models (GAM) fit to each station. The dashed lines are the predicted seasonal peak migration date (highest modeled intensity) for each NEXRAD station. Right inset shows the locations of all seven NEXRAD stations. GAM prediction lines, dashed peak prediction lines, and station locations are shaded according to the station longitude. Both calendar dates (non-leap year) and ordinal dates shown on the x-axis and labeled on the dotted lines.

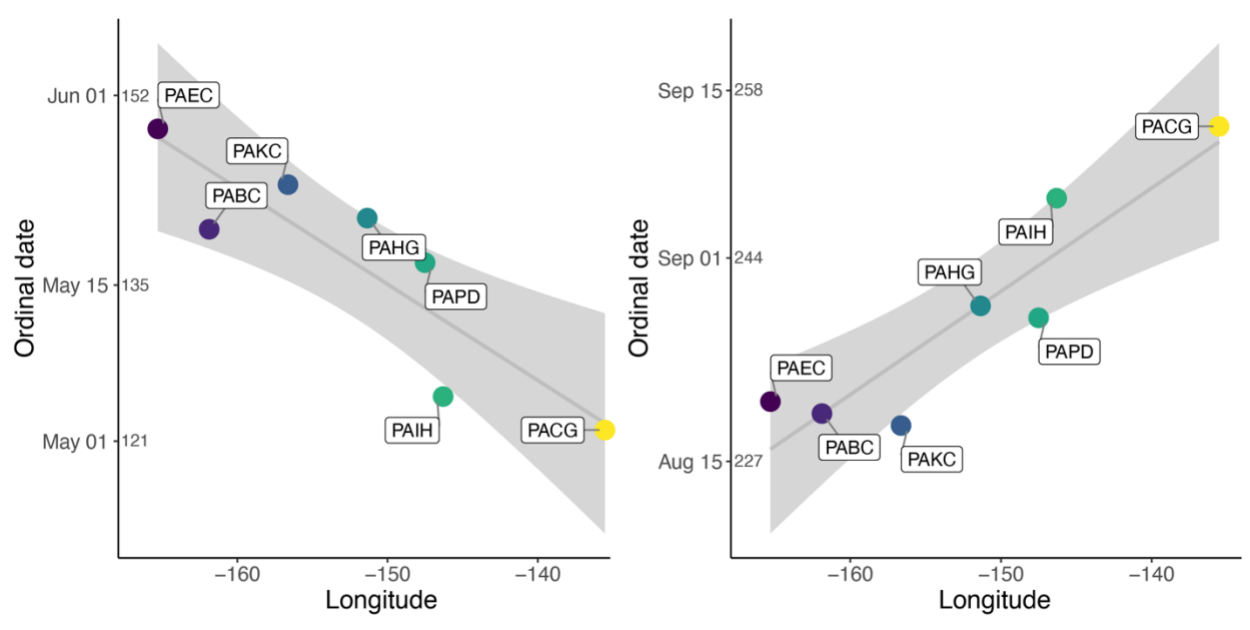


**Figure 3: (A)** Spring and **(B)** fall peak migration dates versus NEXRAD station longitude. Fitted line and 95% confidence interval are from a least squares linear model (spring, slope=0.861, R<sup>2</sup>=0.79, p=0.008; fall, slope=0.862, R<sup>2</sup>=0.84, p=0.004). Point colors corresponds to NEXRAD station longitude. Both calendar dates (non-leap year) and ordinal dates shown on the y-axis.

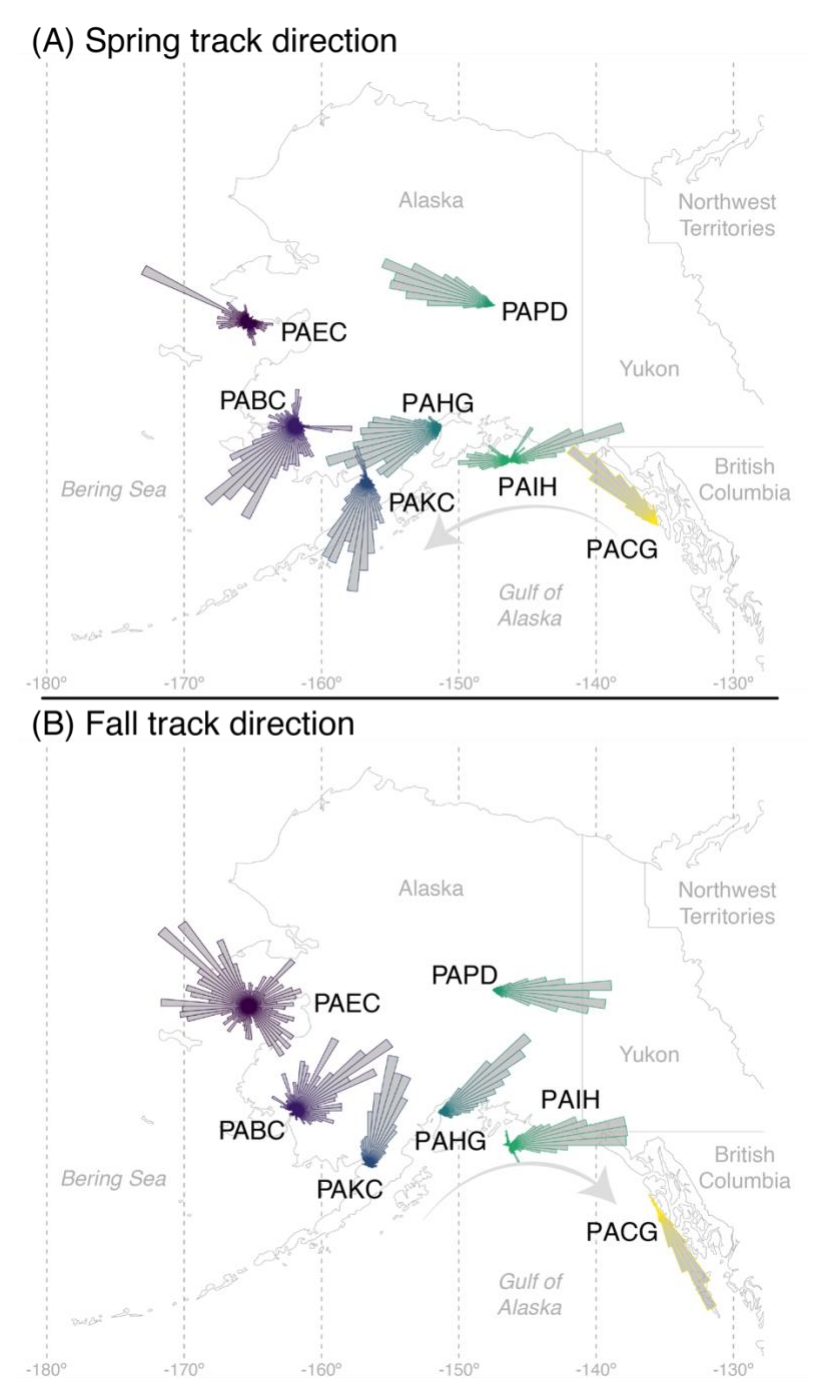


**Figure 4: (A)** Spring and **(B)** fall rose diagrams displaying migrant track direction at each NEXRAD station. Track directions from individual radar scans are represented in rose diagrams, and directions are weighted by reflectivity. All distributions are plotted to show the same maximum size; however, data density varies across each of the stations (see Figure S1). Rose diagrams display 5° summary segments. Intensity measures at PEAC were consistently low, and thus directional observations may be subject to error.

**Table 1:** Seasonal migration dates (q10, peak, and q90), mean track direction, and rho (a measure of track concentration, 0 = no directional concentration, 1= complete directional concentration) at seven Alaskan NEXRAD stations. Calendar dates are shown (non-leap year) followed by ordinal dates in parentheses.

Radar ID	Location	Season	Beginning of migration (q10)	Peak date of migration	End of migration (q90)	Days between spring and fall date of peak migration	Mean track direction (°)	rho
PABC	Bethel	Spring	April 29 <sup>th</sup> (119)	May 20th (140)	June 7 <sup>th</sup> (158)	89	219.76	0.45
		Fall	August 2 <sup>nd</sup> (214)	August 18 <sup>th</sup> (230)	September 15th (258)		48.19	0.56
PACG	Sitka	Spring	April $12^{th}(102)$	May 2nd (122)	May 27th (147)	131	316.57	0.89
		Fall	August 14th (226)	September 11 <sup>th</sup> (254)	October 2 <sup>nd</sup> (275)		152.16	0.66
PAEC	Nome	Spring	April 22nd (112)	May 29th (149)	June 17 <sup>th</sup> (168)	81	265.27	0.27
		Fall	July 31st (212)	August 19 <sup>th</sup> (231)	September 25th (268)		317.36	0.13
PAHG	Anchorage	Spring	April 25 <sup>th</sup> (115)	May 21st (141)	June 8 <sup>th</sup> (159)	97	257.18	0.83
		Fall	August 10th (222)	August 27 <sup>th</sup> (239)	September 14th (257)		62.44	0.84
PAIH	Middleton Island	Spring	April 10 <sup>th</sup> (100)	May 5 <sup>th</sup> (125)	June 2 <sup>nd</sup> (153)	122	20.82	0.21
		Fall	August 12th (224)	September 5 <sup>th</sup> (248)	October 2 <sup>nd</sup> (275)		80.02	0.74
PAKC	King Salmon	Spring	May 1st (121)	May 24th (144)	June 7 <sup>th</sup> (158)	84	197.52	0.65
		Fall	August 4th (216)	August 17 <sup>th</sup> (229)	September 4 <sup>th</sup> (247)		20.50	0.80
PAPD	Fairbanks	Spring	May 2 <sup>nd</sup> (122)	May 17 <sup>th</sup> (137)	May 30 <sup>th</sup> (150)	100	290.48	0.92
		Fall	August 13th (225)	August 26 <sup>th</sup> (238)	September 11 <sup>th</sup> (254)		92.49	0.95

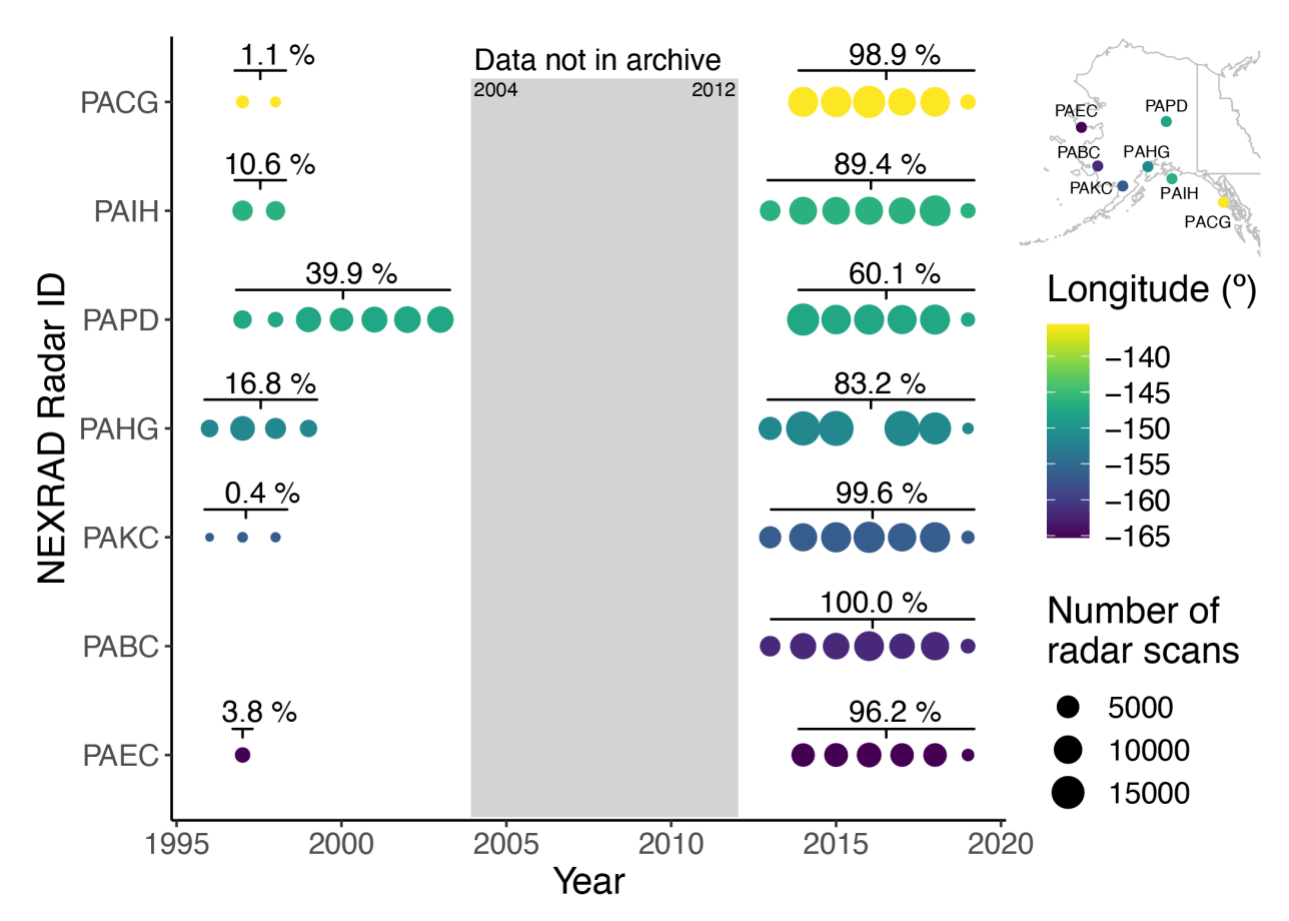


**Figure S1:** Data density for each NEXRAD station. Points within the plot are scaled to the number of annual radar scans from April  $1^{\text{st}}$  to October  $15^{\text{th}}$ , with points shaded by their respective longitude. Data were not archived from 2004 to 2012, so they were not available for our analyses. Percentages show the proportion of total scans pre-2004 and post-2012.

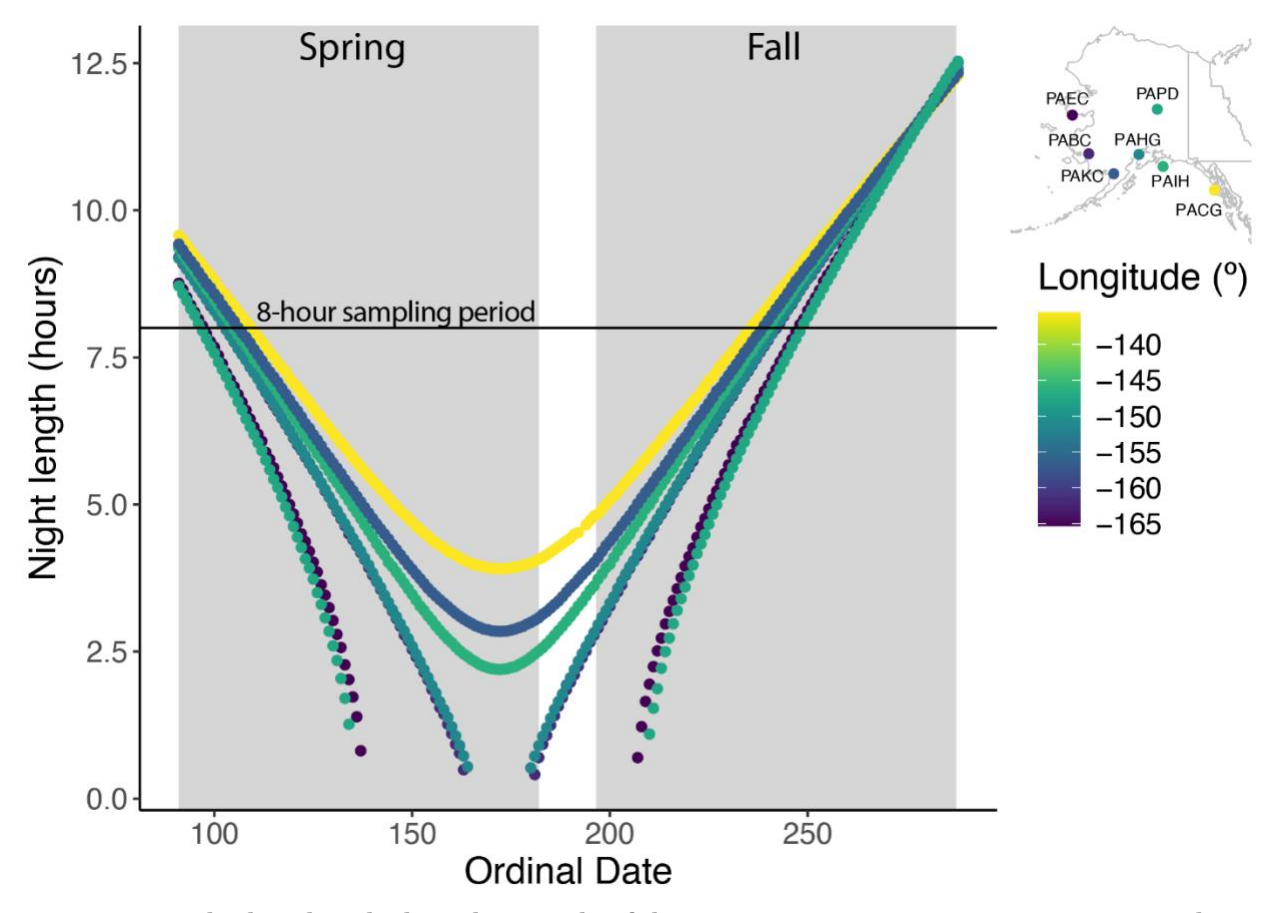


**Figure S2:** Calculated night length at each of the seven NEXRAD stations. For our analysis, we sampled 8-hours of radar scans following the local evening civil twilight (sun 6° below horizon) for any ordinal date with a nocturnal period less than 8-hours. Points shaded by their respective station longitude.

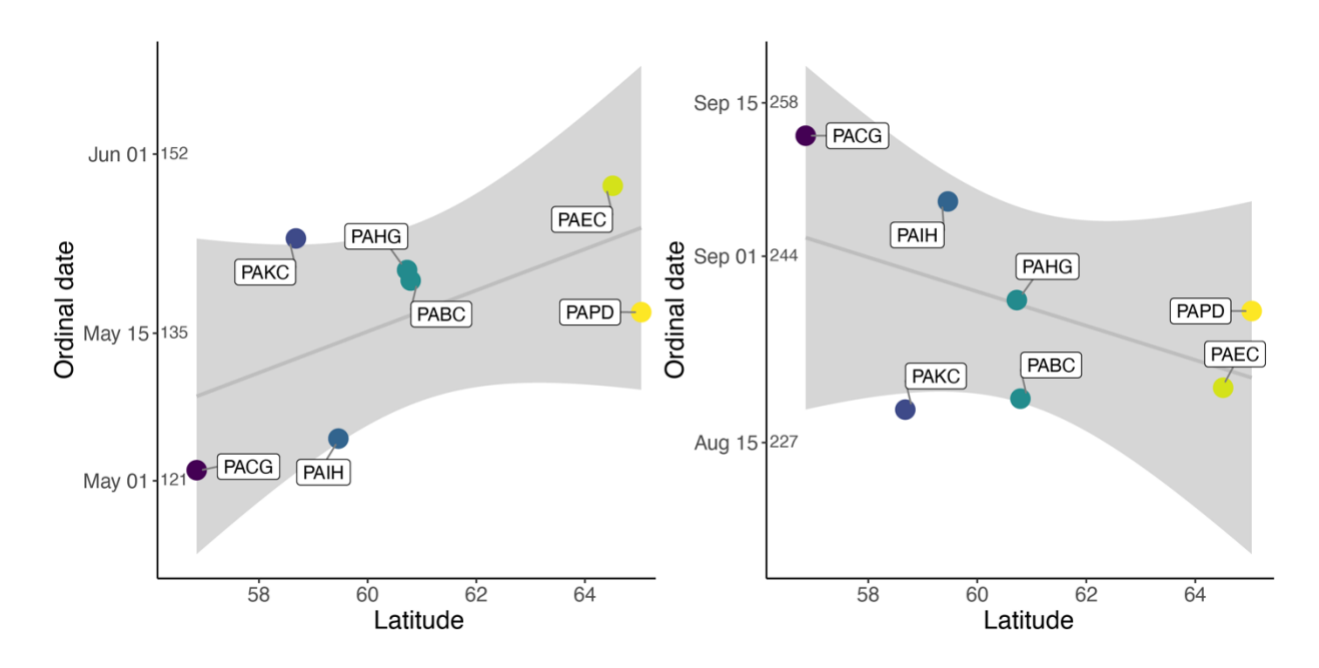


**Figure S3**: (A) Spring and **(B)** fall peak migration date versus NEXRAD station latitude. Fitted line and 95% confidence interval are from a least squares linear model, however both models show non-significant fits (spring,  $R^2$ =0.35, p=0.163; fall,  $R^2$ =0.24, p=0.267). Points correspond to NEXRAD station longitude. Both calendar dates (non-leap year) and ordinal dates shown on the y-axis.